

Epidemic extinction in networks: Insights from the 12,110 smallest graphs

Petter Holme*

*Institute of Innovative Research, Tokyo Institute of Technology,
Nagatsuta-cho 4259, Midori-ku, Yokohama, Kanagawa, 226-8503, Japan*

Liubov Tupikina

*Laboratoire de Physique de la Matière Condensée (UMR 7643),
CNRS – Ecole Polytechnique, 91128 Palaiseau, France*

We investigate the expected time to extinction in the susceptible-infectious-susceptible (SIS) model of disease spreading. Rather than using stochastic simulations, or asymptotic calculations in network models, we solve the extinction time exactly for all connected graphs with three to eight vertices. This approach enables us to discover scaling relations that would be inaccessible with stochastic simulations since the time to extinction, even for small graphs, could be extremely long for even moderate transmission rates. It also enables us to discover graphs and configurations of S and I with anomalous behaviors. We find that for large transmission rates the extinction time is independent of the configurations (of S and I), just dependent on the graph. In this limit, the number of vertices and edges determine the extinction time very accurately (deviations primarily coming from the fluctuations in degrees). We find that, the rankings of configurations (of S and I) with respect to extinction times at low and high transmission rates are correlated at low prevalences and negatively correlated for high prevalences. The most important structural factor determining this ranking is the degrees of the infectious vertices.

I. INTRODUCTION

The susceptible-infectious-susceptible (SIS) model is the canonical model of infectious diseases that leave people re-susceptible to the disease upon recovery. As other compartmental models of infectious diseases [1, 11], it consists of two main components. First, a local description of how the disease spreads between pairs of people, and dies. A susceptible individual in contact with an infectious individual becomes infectious with a rate β ; infectious persons become susceptible again with a rate ν . Second, every epidemic model also describes how people come in contact with each other. Traditionally, one have assumed a fully-connected, or well-mixed, scenario—that anyone can meet anyone else with the same chance at all times. Lately, it has become popular to assume the population is connected into a network and everyone connected by an edge have equal probability of meeting one another, while pairs with no edge will never meet.

Research on the SIS model typically focuses on one of three questions. First, in a finite population (usually assuming the fully-connected scenario) how long time does it take for the outbreak to die out [25, 27]? Second, in an infinite population, there will be a threshold value of β (given ν) below which the outbreak inevitably dies out and above which it can live forever. This line of research investigates how the network structure—the probability distribution of degree (the number of neighbors), the number of triangles, etc.—affects the threshold [28]. In almost all cases (Ref. [13] being an exception) authors have explored the large-size limit by stochastic simulations or approximative calculations. Other questions include the ranking of important vertices with respect to the outbreak [29] and the chains of events that are most likely to lead to extinction [12]

In this work, we will investigate a mix of the questions above. Namely how the network structure and the position of infectious vertices affect extinction in small connected graphs. To our knowledge, this is the first study to investigate the time to extinction from different configurations (of who is susceptible and who is infectious). Scanning small graphs, however, has occasionally been used in network science [14, 17, 21]. Rather than addressing these questions with stochastic simulations, we calculate the exact expression for the expected time to extinction as a function of β (we set $\nu = 1$ without loss of generality). This approach is computationally expensive, so we restrict ourselves to graphs of eight vertices or less. On the other hand, we go through every distinct such graph; 12,110 in total. By distinct, we mean that there are no pair of graphs in this data such that one can relabel the vertices of one to get the other.

Our non-stochastic computational approach makes it possible to discover exact relations among small graphs, such as: what the smallest graph is such that the ranking of configurations' extinction times is independent of β . We can also discover scaling relations, that of course will be hypotheses, but probably hard to find with stochastic approaches since the time to extinction for large β is prohibitively long, also for very small networks [25]. One can make a case for the study of small graphs in some cases. Animal trade networks [2] could be represented as a graph where the nodes are farms (technically speaking metapopulations). These are often small by design, to contain pathogens.

In the rest of the paper, we will describe our approach, in parallel working with one example and introducing the general theory. Then we will go through the numerical findings, first in the limit of large β and finally study how the ranking of configurations depend on β .

* holme@cns.pi.titech.ac.jp

II. PRELIMINARIES

A. The SIS model

Assume a graph $G = (V, E)$ with N vertices labeled from 0 to $N - 1$. Let ϕ_i be a binary state variable ($\phi_i \in \{0, 1\}$). We will interpret $\phi_i = 0$ as vertex i being susceptible while $\phi_i = 1$ means that i is infectious. In the common formulation of the SIS model [7], the probability of a susceptible vertex i being infected by an infectious neighbor j is β per time unit, independent of when j was infectious. Likewise, the recovery of j is time independent, leading to an exponential distribution of the duration of infections. Without loss of generality, we can take the recovery rate to unity. This lack of memory (i.e. Markov property) means that we can encode the current situation of the outbreak into a number $s \in [0, 2^N - 1]$ as $\sum_{i=0}^{N-1} \phi_i 2^i$. We will refer to s as a *configuration* of vertex states.

Now we will proceed to set up the equations for the expected time to extinction from a certain configuration. The derivation closely follows the derivation of the master equations (or Kolmogorov equations) giving the probability of the system being in a certain configuration [7, 18]. We thus effectively treat the SIS dynamics as a random walk in the space of configurations s , where $s = 0$ is an absorbing configuration [22].

Now let $I(s)$ be all configurations reachable from s by an infection event and $S(s)$ the set of configurations reachable from s by a recovery. Let $\omega_s = |S(s)|$ be the number of infectious vertices, a.k.a. the *prevalence*. Let m_{st} be the number of edges between an infectious vertex in configuration s and the vertex that is susceptible in s and infectious in t (with our encoding of configurations, this vertex is $\log_2(t - s)$). Because of the exponential distribution of the durations in the susceptible and infectious states, the rates of events are additive. The total event rate $z_s(\beta)$ is

$$z_s(\beta) = \beta \sum_{t \in I(s)} m_{st} + \omega_s, \quad (1)$$

giving the expected duration of configuration s as $1/z_s(\beta)$. The probability that the next configuration becomes t via a infection event is $\beta m_{st}/z_s(\beta)$, while the probability of the next configuration t reachable through a recovery event is $1/z_s(\beta)$, see Fig. 1.

B. Expected time to extinction

Let x_s denote the expected time to extinction from configuration s . We can write down self-consistency equations for x by noting it is the expected life time of the configuration s , $T_s = 1/z_s(\beta)$, plus the expected extinction times of the configurations reachable from s times their transition probabilities. Symbolically:

$$x_s = T_s + \sum_t x_t \times \text{Prob}(s \rightarrow t), s \in [1, 2^N - 1]. \quad (2)$$

From the above discussion, we get the self-consistency equations (simplified by multiplying both sides of the equations by

$$z_s(\beta))$$

$$z_s(\beta)x_s = 1 + \beta \sum_{t \in I(s)} n_{st}x_t + \sum_{t \in S(s)} x_t, s > 0 \quad (3a)$$

$$x_0 = 0 \quad (3b)$$

where $s \in [0, 2^N - 1]$. From the above equation we can write the equation in the matrix form

$$\mathbf{U}(\beta)\mathbf{x} + \mathbf{1} = 0 \quad (4)$$

where $\mathbf{1} = (1, \dots, 1)^T$, $\mathbf{x} = (x_0, \dots, x_{2^N-1})$, and $\mathbf{U}(\beta)$ is a *polynomial matrix* [9] (since some of the its elements depend on β parameter) defined by:

$$U_{st}(\beta) = \begin{cases} 1 & \text{if } s - t = 2^i, i \in V \\ \beta n_{st} & \text{if } s \neq 0 \text{ and } t - s = 2^i, i \in V \\ -z_s(\beta) & \text{if } s = t \\ 0 & \text{otherwise} \end{cases} \quad (5)$$

where we use the property that $s - t = 2^i, i \in V$, if and only if the only difference between s and t is that vertex with number i is infectious in s and susceptible in t .

Extending Eq. (3) for all configurations s generates a linear system of equations with as many equations as unknowns. We can thus solve it (we use Gaussian elimination in favor of more elaborate methods [23]) to get the expectation value of the extinction times from any initial configuration s .

For the example in Fig. 1, Eqs. (3) become:

$$(\beta + 1)x_1 = 1 + \beta x_3 \quad (6a)$$

$$(2\beta + 1)x_2 = 1 + \beta x_3 + \beta x_6 \quad (6b)$$

$$(\beta + 2)x_3 = 1 + x_1 + x_2 + \beta x_7 \quad (6c)$$

$$(\beta + 1)x_4 = 1 + \beta x_6 \quad (6d)$$

$$(2\beta + 2)x_5 = 1 + x_1 + x_4 + 2\beta x_7 \quad (6e)$$

$$(\beta + 2)x_6 = 1 + x_2 + x_4 + \beta x_7 \quad (6f)$$

$$3x_7 = 1 + x_3 + x_6 + x_5, \quad (6g)$$

where we have omitted the trivial $x_0 = 0$. One can reduce this equation system further by grouping automorphically equivalent configurations (i.e. configurations that can be mapped to one another by a relabeling of the vertices) [31]. In the example of Fig. (1), configurations 1 and 4, and 3 and 6, form two automorphic equivalence classes. This reduces the equation system to:

$$(\beta + 1)x_{1,4} = 1 + \beta x_{3,6} \quad (7a)$$

$$(2\beta + 1)x_2 = 1 + 2\beta x_{3,6} \quad (7b)$$

$$(\beta + 2)x_{3,6} = 1 + x_{1,4} + x_2 + \beta x_7 \quad (7c)$$

$$(2\beta + 2)x_5 = 1 + 2x_{1,4} + 2\beta x_7 \quad (7d)$$

$$3x_7 = 1 + 2x_{3,6} + x_5, \quad (7e)$$

which, furthermore, gives a reduced version of \mathbf{U} that we call \mathbf{Y}

$$\mathbf{Y}(\beta) = \begin{bmatrix} -\beta - 1 & 0 & \beta & 0 & 0 \\ 0 & -2\beta - 1 & 2\beta & 0 & 0 \\ 1 & 1 & -\beta - 2 & 0 & \beta \\ 2 & 0 & 0 & -2\beta - 2 & 2\beta \\ 0 & 0 & 2 & 1 & -3 \end{bmatrix}. \quad (8)$$

Eq. (4) holds with U replaced by Y . Some properties of this matrix matrix include:

1. Below the diagonal, all elements are β independent.
2. Above the diagonal, the elements are integers times β .
3. At each row, except the last (corresponding to the all-infectious configuration) there are two β -dependent elements. The constant coefficients of these terms sum to zero.
4. The diagonal is such that rows sum to zero, except the rows representing states that can reach $s = 0$ by one recovery event, then the row sum is -1 .

Moreover, we note that the number of automorphic equivalence classes n defines the rank of the reduced matrix.

Our example system in Eq. (7) has the solution:

$$x_{1,4} = \frac{4\beta^4 + 16\beta^3 + 35\beta^2 + 34\beta + 12}{16\beta^2 + 28\beta + 12} \quad (9a)$$

$$x_2 = \frac{4\beta^4 + 18\beta^3 + 42\beta^2 + 40\beta + 12}{16\beta^2 + 28\beta + 12} \quad (9b)$$

$$x_{3,6} = \frac{4\beta^4 + 20\beta^3 + 51\beta^2 + 53\beta + 18}{16\beta^2 + 28\beta + 12} \quad (9c)$$

$$x_5 = \frac{4\beta^4 + 20\beta^3 + 53\beta^2 + 52\beta + 18}{16\beta^2 + 28\beta + 12} \quad (9d)$$

$$x_7 = \frac{4\beta^4 + 20\beta^3 + 57\beta^2 + 62\beta + 22}{16\beta^2 + 28\beta + 12}. \quad (9e)$$

The expressions for x_2 and $x_{3,6}$ can be further simplified, but for comparison, we keep the same denominator.

C. Algebraic calculations

Solving Eq. (4) is computationally complex. The major bottleneck is the polynomial algebra (to be precise—calculating the greatest common divisor needed to reduce the fractions of polynomials to their canonical form). The code was implemented in C with the FLINT library [10] for polynomial algebra. To group automorphically equivalent configurations, it also relies on the subgraph isomorphism algorithm VF2 [5] as implemented in the igraph C library [6]. Finding subgraph isomorphisms—although a classical, computationally hard problem—is in practice relatively quick and this enables us to discover and exploit all symmetries rather than *a priori* focusing on symmetrical graphs (cf. Ref. [18]).

Our code is available at github.com/pholme/sis_exact/.

D. Small distinct graphs

We systematically evaluate small distinct (non-isomorphic) connected graphs of sizes up to 8 vertices: $3 \leq N \leq 8$. There are two such graphs with $N = 3$, six with $N = 4$, 20 with $N = 5$, 112 with $N = 6$, 853 with $N = 7$ and 11,117 with

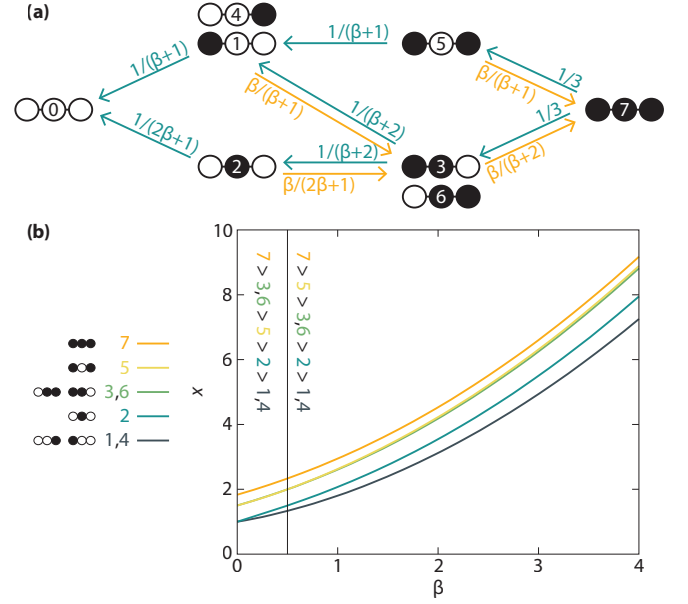


FIG. 1. (Color online) Panel (a) shows the four equivalence classes of configurations of the SIS model at a triangle. The values on arrows gives the transition probabilities. Arrows and probabilities for equivalent configurations (1 and 4, and 3 and 6) are only shown for one of the configurations. Configuration 0 is absorbing—no arrows lead out from it. Panel (b) shows the expected extinction times x derived from (a) as a function of the infection rate β . The vertical line at $\beta = 1/2$ shows where configuration 5 start having a longer expected extinction time than configurations 3 and 6.

$N = 8$, in total, 12110 graphs for $3 \leq N \leq 8$ vertices. To generate these, we use the program Geng [24].

E. Kendall's τ

We compare several types correlations (e.g. between structural measures and times to extinction) in this work. To do that, we will consistently use Kendall's τ correlation coefficient. It is defined as the fraction of pairs connected by a line with a positive slope, minus the fraction of pairs connected by a negative slope [19]. If its value is $+1$, there is a perfect correlation between the ranks of all data points; if the value is -1 , there is a perfect anti-correlation; $\tau = 0$ represents no correlation. We use this coefficient rather than other popular ones for three reasons. First, the output data is typically not Gaussian, so the premises for Pearson's correlation coefficient is violated. Second, to reduce the disk space usage we do not store the explicit expressions of \mathbf{x} , but rather the order of them in the large and small β limits. Third, the number of data points is small enough to use Kendall's τ rather than the faster, but less principled, Spearman rank correlation coefficient.

III. RESULTS

A. An example

We start the discussion of our results by examining the example of Section II B and Fig. 1. Many properties of the solution, Eqs. (9), hold also for other N .

First, in the small limit of β , the solutions are the harmonic numbers of ω_s . This follows immediately from the dynamics defined above—all events are recovery events, the time to the next event is $1/\omega_t$, where ω_t decreases by one every event, leading to the harmonic number $\sum_{t=1}^s 1/\omega_t$.

Second, as $\beta \rightarrow \infty$, the extinction time approaches $u\beta^{N-1}$. For all graphs we study, u is independent of s but dependent on graph structure G . Below, we examine this property in general.

B. Solving our example with Cramer's rule

In this section, we go over an analytical solution by Cramer's rule that gives some insight about the emergence of scaling behavior $u\beta^{N-1}$. Let us derive this exponent for Eq. (9). To do this, we apply Cramer's rule to the polynomial matrix $\mathbf{Y}(\beta)$ denoted further as \mathbf{Y} (we will drop the β argument for most of the derivation below). Cramer's rule states that the s 'th element of vector \mathbf{x} from Eq. (4) is

$$x_s = \frac{\det \mathbf{Y}^s}{\det \mathbf{Y}}, \quad (10)$$

where \mathbf{Y}^s is a matrix obtained from \mathbf{Y} by replacing the s 'th column by the vector $-\mathbf{1}$ (i.e. all elements being minus one).

Let us consider $x_{1,4}$ for our example above (x_1 is also solution x_4 due to symmetric properties). We will use the row and column indices of \mathbf{Y} in this section.

In order to calculate the polynomial degree of determinant of matrix \mathbf{Y}^s we first make a subfactor expansion along the first column of matrix \mathbf{Y} . This gives the expressions:

$$\det \mathbf{Y} = (-\beta - 1)M_{11} + M_{31} - 2M_{41} \quad (11a)$$

$$\det \mathbf{Y}^1 = -M_{11} + M_{21} - M_{31} + M_{41} - M_{51} \quad (11b)$$

where M_{st} is the determinant of the matrix \mathbf{Y} without s 'th row and t 'th column (i.e. the st -minor of \mathbf{Y}). We find that

$$M_{11} = 12\beta^2 + 22\beta + 12 \quad (12a)$$

$$M_{21} = -4\beta^2 - 6\beta \quad (12b)$$

$$M_{31} = 8\beta^3 + 16\beta^2 + 6\beta \quad (12c)$$

$$M_{41} = -2\beta^3 - \beta^2 \quad (12d)$$

$$M_{51} = 4\beta^4 + 6\beta^3 + 2\beta^2, \quad (12e)$$

giving (via Eq. (11a)):

$$\det \mathbf{Y} = -16\beta^2 - 28\beta - 12 \quad (13a)$$

$$\det \mathbf{Y}^1 = -4\beta^4 - 16\beta^3 - 35\beta^2 - 34\beta - 12, \quad (13b)$$

which is in agreement with the numerical results from Eq. (9).

C. Asymptotic scaling: exact relations

We will show that the leading term of x_s is $u\beta^c$ for a c , which for our graphs is connected to the number of nodes: $c = N - 1$. We believe this holds in general, but we have to leave a proof of that for the future.

From Eq. (10), we see that our assertion will be true if we can show that the leading term of $\det \mathbf{Y}^s$ is independent of s . In the Appendix, we show that the determinants of the ns -minors of \mathbf{Y} (cf. Eq. (13b)) have leading terms of polynomial degree $n - 1$ and the same prefactor, independent of s . Such a large polynomial degree is impossible to attain for st -minors with $s < n$, since they have rows not containing any β , some of the $n - 1$ factors of the Leibniz expansion of the determinant must have polynomial degree zero with respect to β . Thus the leading behavior of $\det \mathbf{Y}^s$ comes from M_{ns} and is unique. Since $\det \mathbf{Y}$ is trivially independent of s , the leading behavior of x_s is also s -independent. If $c = N - 1$, we can conclude that $\det \mathbf{Y} = n - N + 1$.

For our example graph (and some other simple graphs of $N \leq 4$ we check) it holds that

$$\deg(M_{st}) = n - N + \omega_s, \quad (14)$$

for all t . If this is true in general, then, curiously, $\det \mathbf{Y}$ is determined by the minors corresponding to the configurations with lowest prevalence and $\det \mathbf{Y}^s$ the one with the highest prevalence. This is somewhat reminiscent of current-flow networks where the determinant of the st -minor of the adjacency matrix is proportional to the potential drop between s and t [4].

D. Numerical results for the large β asymptotics

As mentioned above, the $\beta \rightarrow \infty$ behavior is the same for all the configurations s , namely $x_s = u\beta^{N-1} + O(\beta)$. In this section, we investigate how the sizes of the graphs control the prefactor u .

As we can see in Fig. 2(a), for a given N , u is a power-law of the number of edges M (keeping in mind that u depends on the graph structure):

$$u(M) = u_0 M^\alpha. \quad (15)$$

For the graphs we study, the coefficient α and $\ln u_0$ have a close to linear dependence of N (Fig. 2(b) and (c)):

$$u_0 = 126(1) \times 0.0268(2)^{N-1} \quad (16a)$$

$$\alpha = -1.081(2) + 1.168(1)N \quad (16b)$$

where the number in parentheses represents the standard errors in the last digit. Of course, the error estimates are based on the data we have and subjected to small-size effects. In other words it is conceivable that α could be taken as $N - 1$, giving a large- β approximation \hat{x} of the extinction time x :

$$\hat{x}(\beta, N, M) = a(b\beta M)^{N-1} \quad (17)$$

with constants $a \approx 126$ and $b \approx 0.0268$. Note also that there is a weak but consistent bend (negative second derivative) of

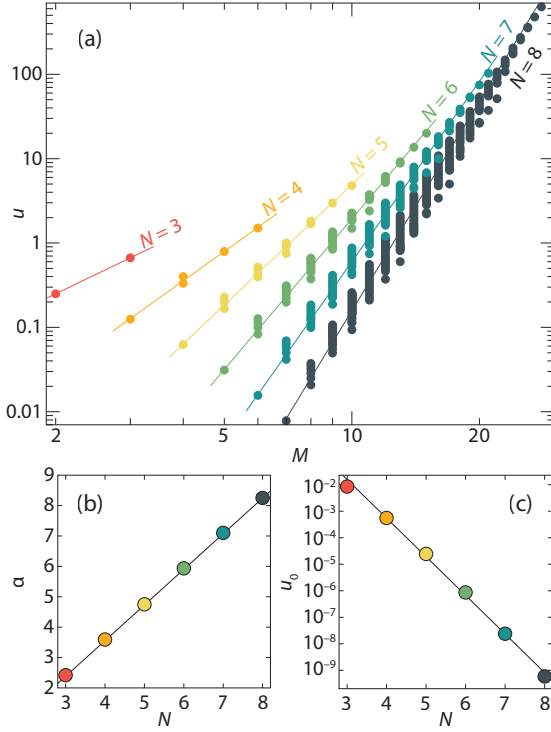


FIG. 2. (Color online) The scaling properties of the asymptote u as a function of the number of edges M . In panel (a), we see a power-law dependence of $u = u_0 M^\alpha$ on the number of edges given the number of vertices. In panels (b) and (c), we see the N dependence of parameters u_0 and α .

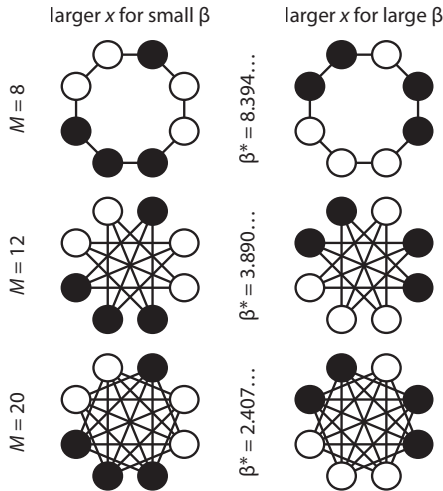


FIG. 3. The only three graphs in our study where all vertices are in equivalent positions but the ranking of configurations (in order of extinction time) depends on β . Black represents infectious; white represents susceptible. β^* gives the β value where the two configurations have the same expected extinction time.

TABLE I. Correlation between measures characterizing the structure of graphs (beyond the number of vertices and edges) and the large- β .

Measure	Kendall's τ
Clustering coefficient	-0.667
Degree assortativity	0.191
Average distance	-0.309
S.d. of degrees	-0.751

In u_0 as a function of N (i.e. a and b seem to be slowly varying functions of N).

As seen in Fig. 2, $u(G)$ is not completely determined by Eq. (16)—there is also some spread of the points for a given N and M . To understand what causes two graphs of the same N and M to differ, we try several structural predictors: the clustering coefficient (a.k.a. transitivity—the fraction of triangles among all connected subsets of three vertices), the degree assortativity (the Pearson correlation of degrees at either side of an edge), the average distance ($d(i, j)$ —the fewest number of edges of any path between i and j), and the standard deviation of the degree. See Refs. [3, 26] for detailed descriptions of applied measures. For all pairs of N and M , we calculate the correlation between the u and these measures, then we average these values over all graphs. The results, shown in Table I shows that all correlations, except the one with degree assortativity, are negative and the strongest correlation is with the standard deviation of degree σ_k . This means epidemics in graphs with more homogeneous degree sequences tend to last longer in the large β limit. The relationship between u and σ_k is shown explicitly in Fig. 4. Indeed, for every combination of N and M the u vs. σ_k curves are almost always decaying. We highlight the curves with largest range in $\ln u$, and note that these occur for close to maximally dense graphs.

E. Pervasiveness of β -dependent rankings of configurations

Already from Fig. 1, we know that the ranking of configurations with the same number of infectious vertices can depend on β . As it turns out, for all but 20 of the 12,110 graphs we study, there is at least one pair of configurations, where one has a longer expected time to extinction for small β and the other for large β . The exceptions to this are all graphs where all vertices are automorphically equivalent. There are 23 such graphs among the ones we study. The three exceptions to the exceptions—the only configurations among such symmetric graphs with a β -dependent ranking—are shown in Fig. 3. There are some interesting symmetries between these graphs evident from the figure. For example, even though the $M=8$ and $M=20$ graphs are complements to each other—two pairs of vertices in one case has an edge if and only if it does not in the other—the ranking of the configurations (which one is dominant for large vs. small β) is the same. However, we do not have any explanations for this observation. The actual times to extinction are extremely similar between the two configurations. In the $M=8$ case, for example, the numerator of

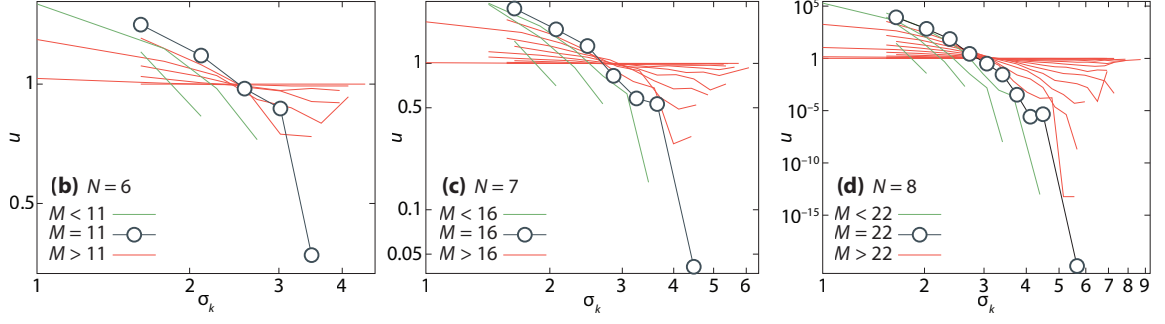


FIG. 4. (Color online) The asymptotic coefficient u as a function of the standard deviation of the degree of the vertices. Different panels represent different number of vertices ($N \geq 6$); different curves represent different number of edges. The curves with the smallest u -values, given N , are highlighted ($M = 11, 16, 22$) as a reference. Note that the axes are logarithmic.

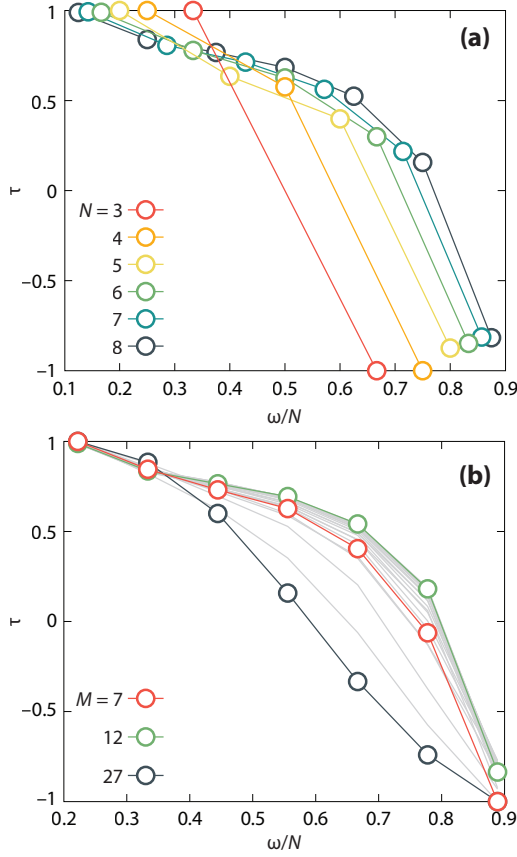


FIG. 5. (Color online) The average correlation (Kendall's τ) of the ranking of configurations in the high and low limits of β as a function of the relative prevalence ω_s/N . Panel (a) shows values averaged over all connected graphs of a certain number of vertices; panel (b) shows the same quantity for $N = 8$ with curves representing averages over graphs with a certain number of edges. The gray curves represent the M values not discussed in the text.

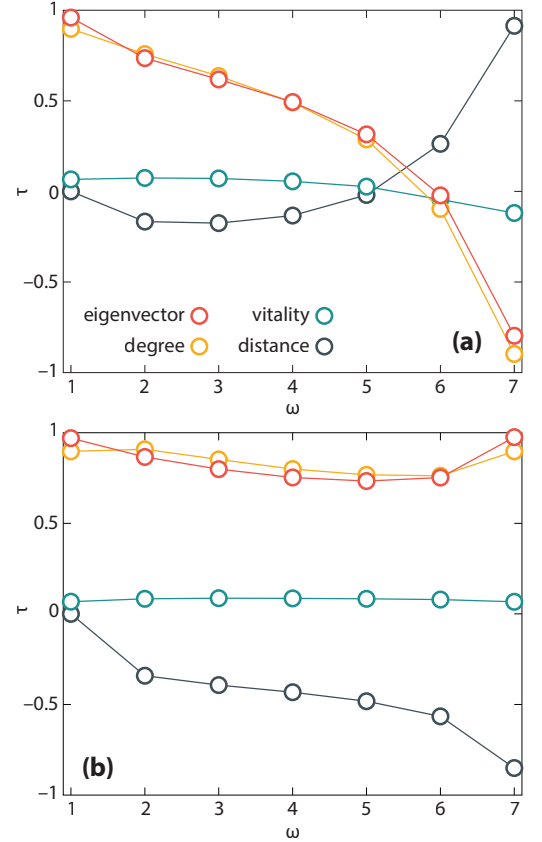


FIG. 6. (Color online) The average correlation (Kendall's τ) between the rank of the configurations at large (a) and small (b) β and various measures of the position of infectious vertices as function of the number ω of infectious vertices. These curves are averaged over all connected graphs with $N = 8$ and $M = 14$ (i.e. with a connectance—fraction of vertex pairs being an edge— $1/2$).

x for the left configuration starts as:

$$\begin{aligned}
 & 97844723712 \times \beta^{28} + 2019406381056 \times \beta^{27} + \\
 & 20485144313856 \times \beta^{26} + 136322491613184 \times \beta^{25} + \\
 & 670461968908288 \times \beta^{24} + \dots
 \end{aligned} \tag{18}$$

while the right configuration has the numerator:

$$97844723712 \times \beta^{28} + 2019406381056 \times \beta^{27} + \\ 20485144313856 \times \beta^{26} + 136322491613184 \times \beta^{25} + \\ 6704\mathbf{55853613056} \times \beta^{24} + \dots \quad (19)$$

(with the differences highlighted by bold face). Needless to say (since they also share the small- β asymptotics) plotting them in the same graph does not show any visible difference. This is an example of a result that would be almost impossible to detect by stochastic simulations.

As N increases, there are more opportunities for symmetry breaking configurations with the same ω_s (below, where it is clear from the context, we write simply ω). One scenario is that for even larger N , the only graphs with β -independent rankings are the fully connected graphs (because for them, all configurations of the same ω are automorphically equivalent and this hence simplifies the system of equations from Section II B). We note that fully connected graphs are the most common interaction structures studied in the literature, and perhaps an unfortunately atypical case.

F. Correlation of asymptotic behaviors

In this section, we continue the investigation of the β -dependence of the rankings of expected extinction times. After calculating \mathbf{x} , we rank the configurations in the limits of large and small β . Let $r_L(s, G)$ be the normalized rank of configuration s among all configurations of the same prevalence I in the large β limit; and $r_S(s, G)$ the corresponding quantity as $\beta \rightarrow 0$. Then we use Kendall's τ coefficient to measure the correlation between r_L and r_S .

In practice, we first put all x_s on the minimal common denominator and compare the numerators (which are polynomials with integer coefficients). To rank polynomials in the small β limit, one first compare the constant coefficient (which is the same for all configurations of the same prevalence), then we use coefficients of increasing polynomial degree as tie-breakers. To rank polynomials as $\beta \rightarrow \infty$, one goes through the coefficients in the opposite direction—one polynomial is considered larger than the other if the highest order coefficient where they differ is larger. As the full equations of the solution for $x_s(\beta)$ take much disk space, we only save the rankings.

With the ranking of the solutions at hand, we proceed to calculate τ (using the NumPy library of Python). In Fig. 5(a), we see τ as a function of the prevalence ω averaged over all connected graphs of given number of vertices $N = 3, \dots, 8$. τ is strictly decreasing from +1 to -1. The decrease (in particular for larger N) is faster in the beginning and end than in the middle. It seems possible that, for yet larger N , this curve would approach a plateau at intermediate values of the prevalence. Stating this in other words, for configurations with few infectious vertices, the ranking is rather independent of β , while for high-prevalence configurations all curves of expected time to extinction will cross as β increases.

In Fig. 5(b), we take a closer look at the $N = 8$ graphs and split the average into different curves depending on the

number of edges. τ has an intermediate maximum for $M = 12$ while the sparsest graph ($M = 7$) has smaller τ than the densest ($M = 27$). For graphs close to the maximum number of edges, the region of slower decrease for small ω is almost gone.

G. Structural determinants of the asymptotic behavior

From the analysis of Fig. 5, we know that the number of vertices and edges affect the ranking of configurations. Now we will look at more detailed explanations based on graph structure—what determines the ranking for graphs of the same N and M ? Fig. 6 presents a case study for $N = 8$ and $M = 14$ (when exactly half of the vertex pairs are connected by an edge).

To measure the correlation, we once again use Kendall's τ . We pick four structural measures to characterize a configuration. Then we correlate each one with either r_S or r_L . We present these measures briefly below. For a thorough account, unless otherwise stated, we refer to Refs. [3, 26].

1. Average *degree*—number of neighbors—of the infectious vertices. Degree is the simplest notion of centrality, but also local (in the sense that a vertex' degree is only dependent on its neighborhood).
2. Average *eigenvector centrality* over the infectious vertices. The eigenvector centrality is given by the eigenvector corresponding to the leading eigenvalue of the adjacency matrix. It is perhaps the most straightforward generalization of degree to account for the idea that being central to central vertices makes a vertex central.
3. Average *vitality* of the infectious vertices. Vitality is the general class of measures based on measuring the response of some graph descriptor on the deletion of a vertex [20]. Following Ref. [14], we define the vitality of vertex i to be $v(i) = [S(G) - 1]/S(G \setminus \{i\})$. Where $S(G)$ denotes the number of vertices of the largest connected component of graph G . This measure will be very close to one for larger graphs and would thus be unsuitable if one were to scale this study up. It is, on the other hand, interesting as it is directly measuring the contribution the presence of a vertex makes in a worst case, $\beta \rightarrow \infty$, scenario.
4. Average *distance* $d(i, j)$ between infectious vertex pairs $i \neq j$. This is the only measure we use that does not involve averaging a centrality measure.

In addition to these we also try the standard measures *betweenness* and *closeness* centrality, but these do not contribute much to the understanding. Partly because they are very correlated with degree and eigenvector centrality for these small graphs, partly because their rationales involves shortest paths—something that disease transmission is not consciously seeking.

In Fig. 6, we plot results of the correlation coefficient between the the above measures of position and the ranks of

the configurations for all connected graphs with $N = 8$ and $M = 14$. Fig. 6(a) shows the case of large β . For configurations with low prevalence, we see that large degree is strongly correlated with the extinction-time ranking. This is natural, since for low β and ω secondary effects are negligible—the number of ways to increase ω counts more than other factors, i.e. the degree. Eigenvector centrality behaves almost like degree. Although not identical, these two quantities are strongly correlated for the small graphs we study, so it is natural the values are close. Somewhat interestingly, which one of these that gives the largest τ varies with β in an irregular way. For sparser graphs (than the one in Fig. 6), that are more prone to disintegrating upon vertex-deletion, vitality shows a correlation on par with degree and eigenvector centrality. Finally, the average distance shows an increasing correlation with ω . That the infectious vertices are far away means that the surface to the susceptible vertices are larger and thus that the next event is more likely to be an infection event.

The structural correlations for the small- β case (Fig. 6(b)) is no surprise in the light of Fig. 5 and Fig. 6(a). Since there is a correlation between r_S and r_L at small ω and a corresponding anti-correlation at large ω , we expect the correlations with structural measures to be similar between the small and large β cases for small ω and different for large ω . This is also rather accurately describing what happens. In this case, the degree and eigenvector centrality are strongly correlated to r_S for all ω , while the distance becomes strongly anti correlated for large ω .

IV. DISCUSSION

We have studied the extinction of SIS epidemics on small graphs. We did so by calculating the exact expressions for the expected time to extinction for all connected graphs between three and eight vertices.

We find that, for a certain graph, the limit behavior as $\beta \rightarrow \infty$ is independent of the configuration of susceptible and infectious, while for $\beta \rightarrow 0$ it is (trivially) just dependent on the number of infectious vertices. The actual asymptotic extinction times u depend on the size and structure of the graph—the time to extinction for large β is proportional to $u_0 M^\alpha \beta^{N-1}$ where both u_0 and α are linear functions of N for the graphs we investigate. This gives a large β scaling of x as $a(b\beta M)^{N-1}$ where $a \approx 126$ and $b \approx 0.0268$. This super-exponential scaling is in line with earlier observations [8, 13, 25, 27]. Simply speaking, even though there is a finite chance of extinction of SIS epidemics in finite graphs, for β only a little more than one, this probability is so small it can be ignored for all practical purposes for all but the smallest graphs. For graphs of the same number of vertices and edges, the strongest determinant of the asymptotic behavior of the time to extinction is the variability (measured by the standard deviation) of the degree. Outbreaks tend to last longer in graphs of heterogeneous degree distributions.

Furthermore, given an interaction graph, we investigated when the ranking of configurations with respect to extinction time shifts with β . For configurations with few infectious ver-

tices, the rankings are typically the same for large and small β ; for configurations with many infectious vertices, there is an anti-correlation between the extinction times in the large and small β limits. The main structural predictors for the rank of configurations with the same number of infectious vertices within the same graph are degree and eigenvector centrality, while the correlations with vitality and inter-vertex distance are weaker.

The main contribution of this paper is to give a view of the relation between graph structure and epidemic behavior from the other end than usual. Rather than studying the $N \rightarrow \infty$ limit by stochastic simulations, we study exact expectation values of small graphs. This enables us to discover hypotheses that could be tested in standard stochastic simulations. It also makes it possible to discover the smallest graphs and configurations with some specific properties. For example, the graph of Fig. 1(a)—where the configurations 3 and 6 have longer extinction times than configuration 5 in the interval $0 < \beta < 1/2$ and vice versa for $\beta > 1/2$ —is the smallest of a graph where configurations change the order of expected extinction time with β . The answer to the reversed question—what is the smallest graph where all same-prevalence configurations are ranked equally for large and small β is the triangle $E = \{(0, 1), (1, 2), (2, 0)\}$. In fact, all graphs where at least two vertices are in different positions (not automorphically equivalent) do not have the equal-ranking property, but 20 of 23 of the graphs we study where all vertices are in the same position do have it.

We anticipate more computational epidemiology studies without random numbers in the future, and simulation studies testing the findings in this work holds for larger graphs. It would also be interesting to go beyond expected times and derive the probability distribution of extinction time. That would need a different computational approach. For a model of networks one could consider mapping the problem to that of mean first-passage times [15, 16, 22], or combinatorial stochastic processes [30].

ACKNOWLEDGMENTS

We thank Naoki Masuda and Petteri Kaski for helpful comments. LT acknowledges the support under Grant No. ANR-13-JSV5-0006-01 of the French National Research Agency.

Appendix A: Leading terms of minors are identical

In this appendix, we will prove that the leading terms of the ns -minors of \mathbf{Y} are the same. For this proof, first recall Leibniz formula for determinants saying that a determinant is a sum of products of matrix elements

$$\prod_{s=1}^n Y_{s\sigma(s)} \quad (\text{A1})$$

where $\sigma(s)$ is a permutation of the numbers to n (the size of \mathbf{Y} , i.e. the number of automorphic equivalence classes of configurations). To calculate the full determinant one needs to

multiply half of the terms by -1 , but we can ignore that for our purpose. We will show that the ns -minors have exactly one term with polynomial degree n equal to the product of the prefactors of β along the diagonal of \mathbf{Y} .

Recalling points 4 and 3 of Section II B, we can write $Y_{ss} = -B_s\beta - A_s$ with $A_s, B_s > 0$ for $s = 1, \dots, n-1$. Furthermore, there is a number $j(s) > s$ such that $Y_{sj(s)} = B_s$. For the special case M_{nn} our results is easy since the nn -minor is upper triangular with respect to elements containing β , and all diagonal elements contain β . Clearly the the leading coefficient is the product of the diagonal, $\prod_{s=1}^{n-1} B_s$, since any other term would contain sub-diagonal elements with polynomial degree zero.

We will solve the case $s < n$ by constructing an algorithm to find the unique leading term of M_{ns} . We will work with the indices of \mathbf{Y} rather than indices of the minor.

1. Set $\Lambda := \{s\}$, $i := j(s)$ and $z := 1$.
2. If $i = n$, go to step 5.
3. Multiply $Y_{ij(i)}$ to z , add i to Λ .
4. Set $i := j(i)$ and go to step 2.

5. For all $i \in \Lambda \cap \{1, \dots, n\}$, multiply Y_{ii} to z .

z , at the exit, is a the term of M_{ns} with highest polynomial degree. First, we note that by construction, z is a product of n elements of the ns -minor of \mathbf{Y} . Then, because the row and column indices are strictly increasing when updated at step 4, no row or column index of an element multiplied by z at step 3 occur twice. Furthermore, this is also true at step 5 (otherwise they such elements would already be multiplied into z are step 3), so z is indeed a term of M_{ns} . It has polynomial degree $n-1$, which is the maximal possible since the maximal polynomial degree of matrix \mathbf{Y} elements is one. Finally, there cannot be any other term of M_{ns} with polynomial degree $n-1$. Step 3 adds factors that must necessarily belong to a term of polynomial degree $n-1$ (since there is only one element containing β at row s). Finally, one cannot multiply by an element $Y_{ij(i)}$ rather than Y_{ii} at step 5, since then z would not include an element from the i 'th column.

Unfortunately, it is not straightforward to extend this algorithm to a proof of Eq. (14). For example, for st -minors with $t < n$, there can be columns without any element containing β meaning that the leading terms (that then will have a polynomial degree less than $n-1$) can contain elements from below of the diagonal \mathbf{Y} . This means that one cannot base proofs about the algorithm on the fact that it samples elements of increasing indices as above.

-
- [1] R. M. Anderson and R. M. May. *Infectious diseases in humans*. Oxford University Press, Oxford, 1992.
 - [2] P. Bajardi, A. Barrat, L. Savini, and V. Colizza. Optimizing surveillance for livestock disease spreading through animal movements. *J. Roy. Soc. Interface*, 9(76):2814–2825, 2012.
 - [3] A.-L. Barabási. *Network Science*. Cambridge Press, Cambridge UK, 2016.
 - [4] R. L. Brooks, C. A. B. Smith, A. H. Stone, and W. T. Tutte. Determinants and current flows in electric networks. *Discrete Mathematics*, 100:291–301, 1992.
 - [5] L. P. Cordella, P. Foggia, C. Sansone, and M. Vento. An improved algorithm for matching large graphs. In *3rd IAPR-TC15 Workshop on Graph-based Representations in Pattern Recognition*, Cuen, pages 149–159, 2001.
 - [6] G. Csárdi and T. Nepusz. The igraph software package for complex network research. *InterJournal Complex Systems*, 1695:1695, 2006.
 - [7] D. J. Daley and J. Gani. *Epidemic modelling: An introduction*. Cambridge University Press, Cambridge, 1999.
 - [8] C. R. Doering, K. V. Sargsyan, L. M. Sander, and E. Vanden-Eijnden. Asymptotics of rare events in birthdeath processes bypassing the exact solutions. *Journal of Physics: Condensed Matter*, 19(6):065145, 2007.
 - [9] F. R. Gantmacher. *The theory of matrices*. Chelsea Pub. Co., New York, 1960.
 - [10] W. B. Hart. Fast library for number theory: An introduction. In *Proceedings of the Third International Congress on Mathematical Software*, ICMS'10, pages 88–91, Berlin, Heidelberg, 2010. Springer-Verlag.
 - [11] H. W. Hethcote. The mathematics of infectious diseases. *SIAM Rev.*, 32(4):599–653, 2000.
 - [12] J. Hindes and I. B. Schwartz. Epidemic extinction paths in complex networks. *Phys. Rev. E*, 95:052317, May 2017.
 - [13] P. Holme. Shadows of the susceptible-infectious-susceptible immortality transition in small networks. *Phys. Rev. E*, 92:012804, Jul 2015.
 - [14] P. Holme. Three faces of node importance in network epidemiology: Exact results for small graphs. *Phys. Rev. E*, 96:062305, 2017.
 - [15] S. Hwang, D.-S. Lee, and B. Kahng. First passage time for random walks in heterogeneous networks. *Phys. Rev. Lett.*, 109:088701, Aug 2012.
 - [16] F. Iannelli, A. Koher, D. Brockmann, P. Hövel, and I. M. Sokolov. Effective distances for epidemics spreading on complex networks. *Phys. Rev. E*, 95:012313, Jan 2017.
 - [17] H. Kim, S. H. Lee, and P. Holme. Building blocks of the basin stability of power grids. *Phys. Rev. E*, 93:062318, Jun 2016.
 - [18] I. Z. Kiss, J. C. Miller, and P. L. Simon. *Mathematics of Epidemics on Networks*. Springer, Heidelberg, Berlin, 2017.
 - [19] W. R. Knight. A computer method for calculating Kendall's tau with ungrouped data. *Journal of the American Statistical Association*, 61:436–439, 1966.
 - [20] D. Koschützki, K. Lehmann, L. Peeters, S. Richter, D. Tenfelde-Podehl, and O. Zlotowski. Centrality indices. In *Network Analysis: Methodological Foundations*, pages 16–61. Springer, Berlin, Heidelberg, 2005.
 - [21] N. Masuda. Directionality of contact networks suppresses selection pressure in evolutionary dynamics. *Journal of Theoretical Biology*, 258(2):323–334, 2009.
 - [22] N. Masuda, M. A. Porter, and R. Lambiotte. Random walks and diffusion on networks. *Physics Reports*, 716-717:1–58, 2017.
 - [23] M. T. McClellan. The exact solution of systems of linear equa-

- tions with polynomial coefficients. *J. ACM*, 20(4):563–588, Oct. 1973.
- [24] B. D. McKay and A. Piperno. Practical graph isomorphism II. *Journal of Symbolic Computation*, 60:94–112, 2014.
- [25] I. Nåsell. Extinction and quasi-stationarity in the Verhulst logistic model. *Journal of Theoretical Biology*, 211(1):11 – 27, 2001.
- [26] M. E. J. Newman. *Networks: An Introduction*. Oxford University Press, Oxford UK, 2010.
- [27] O. Ovaskainen and B. Meerson. Stochastic models of population extinction. *Trends in Ecology & Evolution*, 25(11):643–652, 2010.
- [28] R. Pastor-Satorras, C. Castellano, P. Van Mieghem, and A. Vespignani. Epidemic processes in complex networks. *Rev. Mod. Phys.*, 87:925–979, Aug 2015.
- [29] B. Qu, C. Li, P. Van Mieghem, and H. Wang. Ranking of nodal infection probability in susceptible-infected-susceptible epidemic. *Scientific Reports*, 7:9233, 2017.
- [30] R. Sainudiin and D. Welch. The transmission process: A combinatorial stochastic process for the evolution of transmission trees over networks. *Journal of Theoretical Biology*, 410:137 – 170, 2016.
- [31] P. L. Simon, M. Taylor, and I. Z. Kiss. Exact epidemic models on graphs using graph-automorphism driven lumping. *Journal of Mathematical Biology*, 62(4):479–508, Apr 2011.